Spectral Measurement of Electron Antineutrino Oscillation Amplitude and Frequency at Daya Bay

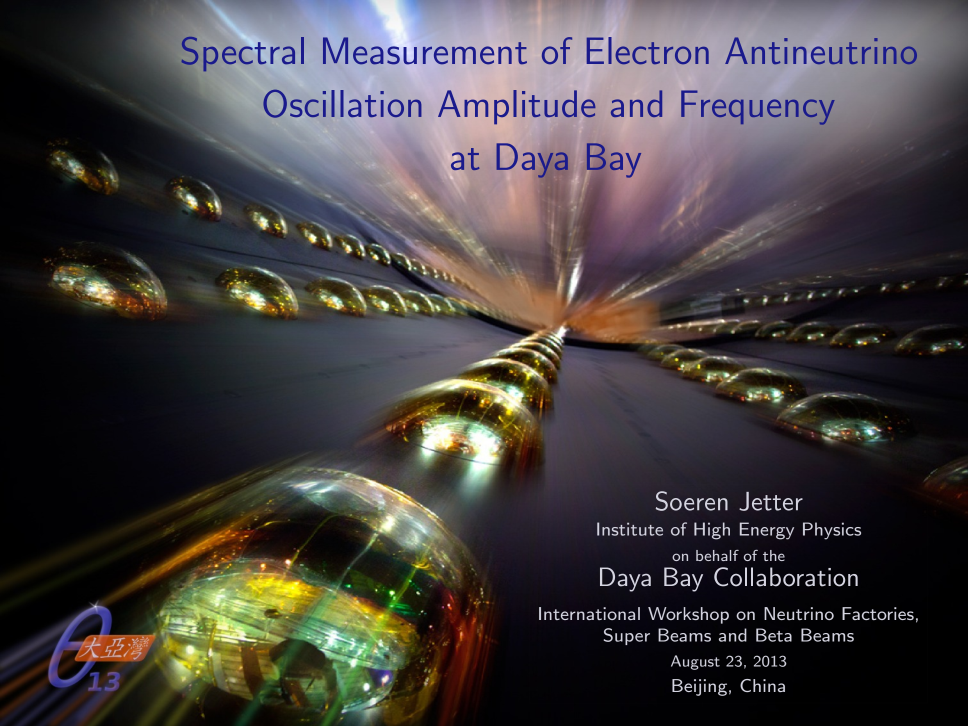

Soeren Jetter
Institute of High Energy Physics
on behalf of the
Daya Bay Collaboration

International Workshop on Neutrino Factories, Super Beams and Beta Beams

August 23, 2013

Beijing, China

Short Baseline Reactor Neutrino Oscillation

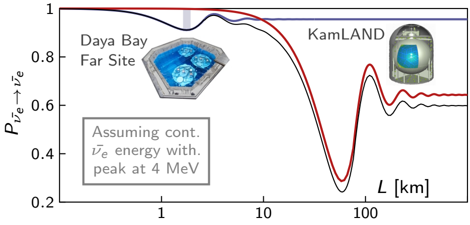

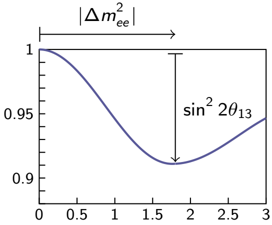

θ_{13} revealed by deficit of reactor antineutrinos at $\sim$ 2 km

$\boxed{1}$ Mixing angle θ_{13} governs overall size of $\bar{\nu}_e$ deficit

$\boxed{2}$ Effective mass squared difference $|\Delta m^2_{ee}|$ determines deficit dependence on L/E

Short Baseline — Long Baseline

$$P_{\bar{\nu}_e \to \bar{\nu}_e} = 1 - \underbrace{\sin^2 2\theta_{13} \sin^2\left(\Delta m^2_{ee} \frac{L}{4E}\right)}_{\text{Short Baseline}} - \underbrace{\sin^2 2\theta_{12} \cos^4 2\theta_{13} \sin^2\left(\Delta m^2_{21} \frac{L}{4E}\right)}_{\text{Long Baseline}}$$

$$\sin^2(\Delta m^2_{ee} \tfrac{L}{4E}) \equiv \cos^2\theta_{12} \sin^2(\Delta m^2_{31} \tfrac{L}{4E}) + \sin^2\theta_{12} \sin^2(\Delta m^2_{32} \tfrac{L}{4E})$$

The Daya Bay Experiment

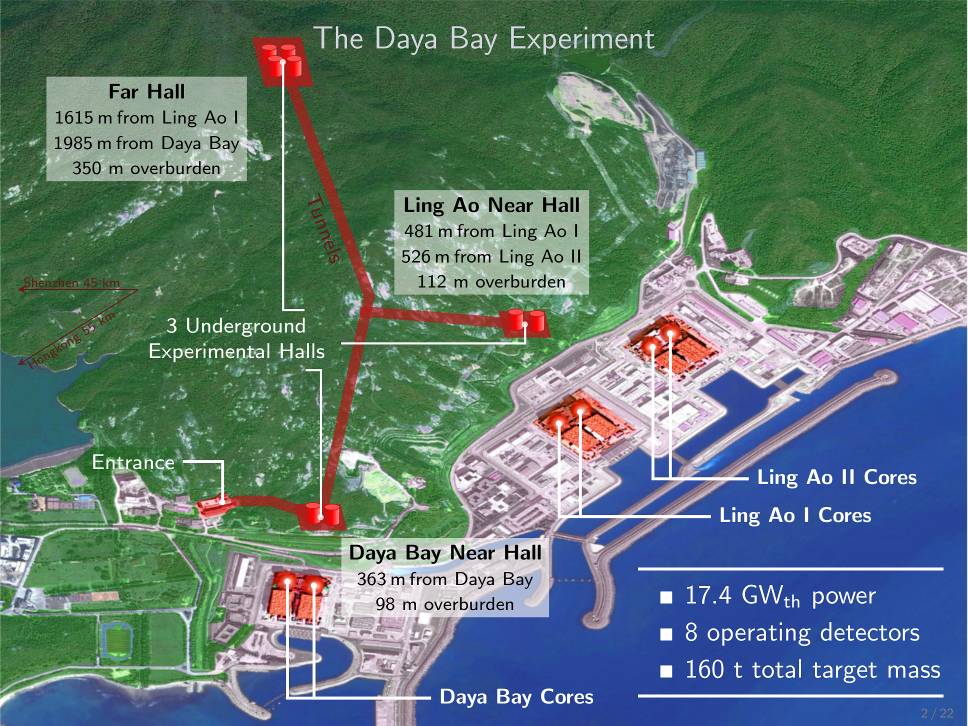

- 17.4 GW_{th} power
- 8 operating detectors
- 160 t total target mass

Daya Bay Calibration System

3 'robots' employed along 3 z-axes

1. Center of GdLS target volume
2. Edge of GdLS target volume
3. Middle of LS gamma catcher volume

3 sources in each robot (employed weekly)

1. ^{68}Ge (2×511 keV γ)
2. ^{241}Am^{13}C (n) + ^{60}Co (1.17+1.33 MeV γ)
3. LED diffuser ball

Additional temporary sources

1. Gamma sources:
   - ^{137}Cs (0.662 MeV)
   - ^{54}Mn (0.835 MeV)
   - ^{40}K (1.461 MeV)
2. Neutron sources
   - ^{241}Am-^{9}Be, ^{239}Pu-^{13}C

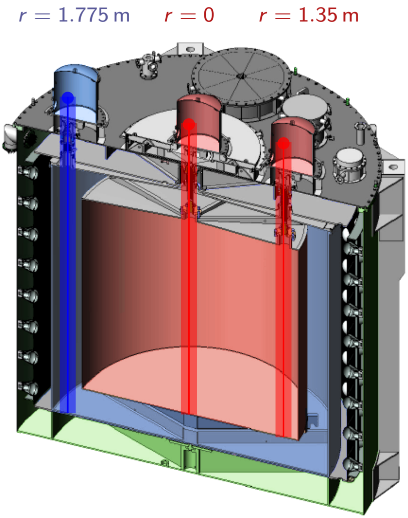

Analyzed Data Sets

Two detector comparison [1202.6181]

- 90 days of data, Daya Bay near only
- NIM A **685** (2012), 78-97

First oscillation analysis [1203:1669]

- 55 days of data, 6 ADs near+far
- PRL **108** (2012), 171803

Improved oscillation analysis [1210.6327]

- 139 days of data, 6 ADs near+far
- CPC **37** (2013), 011001

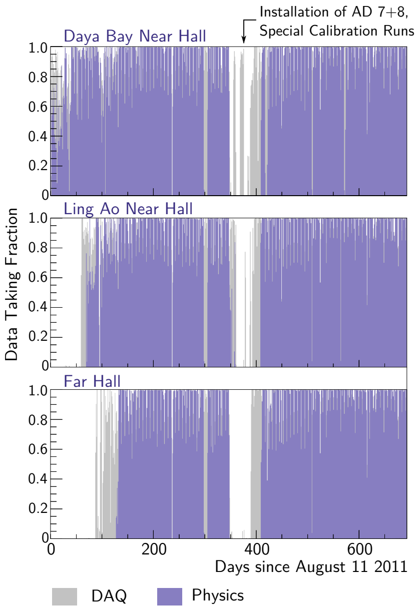

Analyzed Data Sets

Two detector comparison [1202.6181]

- 90 days of data, Daya Bay near only
- NIM A **685** (2012), 78-97

First oscillation analysis [1203:1669]

- 55 days of data, 6 ADs near+far
- PRL **108** (2012), 171803

Improved oscillation analysis [1210.6327]

- 139 days of data, 6 ADs near+far
- CPC **37** (2013), 011001

Spectral Analysis

- 217 days complete 6 AD period
- 55% more statistics than CPC result

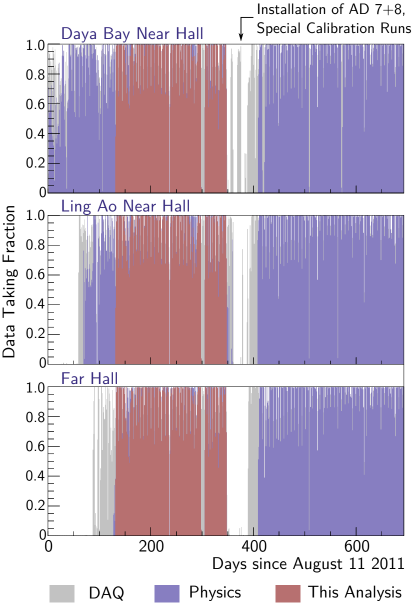

Signal and Background Summary

	Near Halls			Far Hall		
	AD 1	AD 2	AD 3	AD 4	AD 5	AD 6
IBD candidates	101290	102519	92912	13964	13894	13731
DAQ live time (days)	191.001		189.645	189.779		
Efficiency $\epsilon_\mu \cdot \epsilon_m$	0.7957	0.7927	0.8282	0.9577	0.9568	0.9566
Accidentals (per day)*	9.54±0.03	9.36±0.03	7.44±0.02	2.96±0.01	2.92±0.01	2.87±0.01
Fast-neutron (per day)*	0.92±0.46		0.62±0.31	0.04±0.02		
^{9}Li/^{8}He (per day)*	2.40±0.86		1.2±0.63	0.22±0.06		
Am-C corr. (per day)*	0.26±0.12					
^{13}C^{16}O backgr. (per day)*	0.08±0.04	0.07±0.04	0.05±0.03	0.04±0.02	0.04±0.02	0.04±0.02
IBD rate (per day)*	653.30±2.31	664.15±2.33	581.97±2.07	73.31±0.66	73.03±0.66	72.20± 0.66

*Background and IBD rates were corrected for the efficiency of the muon veto and multiplicity cuts $\epsilon_\mu \cdot \epsilon_m$

Collected more than 300k antineutrino interactions

- Consistent rates for side-by-side detectors (expected AD1/AD2 ratio $\sim$ 0.981)
- Uncertainties still dominated by Far Hall statistics $\sim$ 0.9%

Antineutrino Rate vs Time

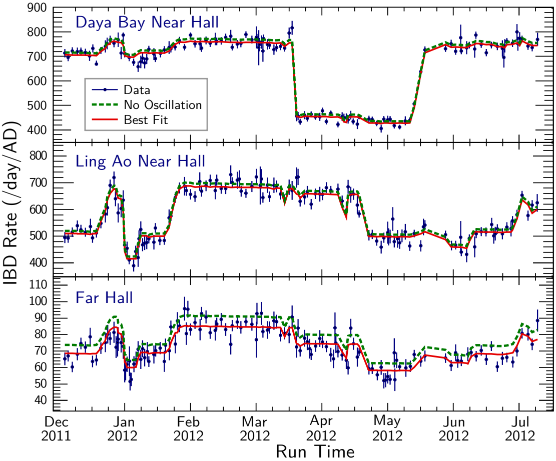

Detected rate strongly correlated with reactor flux expectations

- Predicted Rate assumes no oscillation
- Absolute normalization determined by fit to data
- Normalization within a few percent of expectations

Rate-Only Oscillation Results

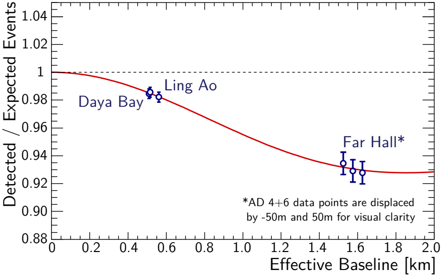

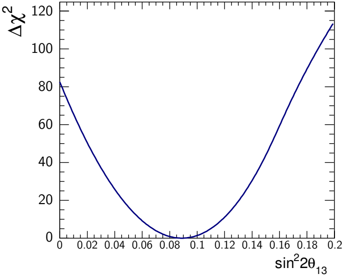

$$\sin^2 2\theta_{13} = 0.089 \pm 0.009$$

- Uncertainty reduced by statistics of complete 6 AD data period
- Standard χ^2 approach: $\chi^2/N_{\text{DoF}} = 0.48/4$
- $|\Delta m^2_{ee}|$ constrained by MINOS: $|\Delta m^2_{\mu\mu}| = 2.41^{+0.09}_{-0.10} \cdot 10^{-3}\text{eV}^2$ [PRL **110**, 251801 (2013)]
- Far vs. near relative measurement: absolute rate not constrained
- Consistent results from independent analyses, different reactor flux models

Spectral Information

Rate-only analysis: previously reported + updated here

$$\frac{N_{\text{far}}}{N_{\text{near}}} = \frac{N_{\text{protons,far}}}{N_{\text{protons,near}}} \frac{L^2_{\text{far}}}{L^2_{\text{near}}} \frac{\epsilon_{\text{far}}}{\epsilon_{\text{near}}} \frac{\int_{E_{\min}}^{E_{\max}} P_{ee}\left(E, L_{\text{far}}; \theta_{13}, \Delta m^2_{ee}\right) \sigma(E)\Phi(E)\, dE}{\int_{E_{\min}}^{E_{\max}} P_{ee}\left(E, L_{\text{near}}; \theta_{13}, \Delta m^2_{ee}\right) \sigma(E)\Phi(E)\, dE}$$

- ✓ Fewer systematic uncertainties
- ✗ Less sensitive, unable to constrain Δm^2_{ee}

Spectral Information

Rate-only analysis: previously reported + updated here

$$\frac{N_{\text{far}}}{N_{\text{near}}} = \frac{N_{\text{protons,far}}}{N_{\text{protons,near}}} \frac{L_{\text{far}}^2}{L_{\text{near}}^2} \frac{\epsilon_{\text{far}}}{\epsilon_{\text{near}}} \frac{\int_{E_{\text{min}}}^{E_{\text{max}}} P_{ee}\left(E, L_{\text{far}}; \theta_{13}, \Delta m_{ee}^2\right) \sigma(E)\Phi(E)\, dE}{\int_{E_{\text{min}}}^{E_{\text{max}}} P_{ee}\left(E, L_{\text{near}}; \theta_{13}, \Delta m_{ee}^2\right) \sigma(E)\Phi(E)\, dE}$$

✓ Fewer systematic uncertainties

✗ Less sensitive, unable to constrain Δm_{ee}^2

Rate+spectrum analysis: to be presented here

$$\frac{\frac{dN_{\text{far}}}{dE}}{\frac{dN_{\text{near}}}{dE}} = \frac{N_{\text{protons,far}}}{N_{\text{protons,near}}} \frac{L_{\text{far}}^2}{L_{\text{near}}^2} \frac{\epsilon_{\text{far}}}{\epsilon_{\text{near}}} \frac{P_{ee}\left(E, L_{\text{far}}; \theta_{13}, \Delta m_{ee}^2\right) \sigma(E)\Phi(E)}{P_{ee}\left(E, L_{\text{near}}; \theta_{13}, \Delta m_{ee}^2\right) \sigma(E)\Phi(E)}$$

✓ Each energy bin independent oscillation measurement, Δm_{ee}^2

✗ Requires detailed understanding of detector energy response

Overview of the Energy Response Model

Particle Energy E_{true}

↓

Energy Losses in Acrylic

Acrylic vessels non-scintillating

- Induce shape distortion
- Correction from MC

Energy Deposited in Scintillator E_{dep}

↓

Scintillator Response

- Quenching effects
- Cherenkov radiation

Energy Converted to Visible Light E_{vis}

↓

Energy Resolution

- Light production
- Light collection
- PMT/electronics response

Readout Electronics

- Charge collection efficiency decreases with visible light

Reconstructed Energy E_{rec}

Model maps reconstructed energy E_{rec} to true kinetic energy E_{true}

- Minimal impact on oscillation measurement
- Crucial for measurement of reactor spectra

Overview of the Energy Response Model

Particle Energy E_{true}

Energy Deposited in Scintillator E_{dep}

Energy Converted to Visible Light E_{vis}

Reconstructed Energy E_{rec}

Energy Losses in Acrylic

Acrylic vessels non-scintillating

- Induce shape distortion
- Correction from MC

Energy Resolution

- Light production
- Light collection
- PMT/electronics response

Two major sources of non-linearity. Difficult to decouple !

Scintillator Response

- Quenching effects
- Cherenkov radiation

Readout Electronics

- Charge collection efficiency decreases with visible light

Total effective non-linearity f

$$f = \frac{E_{rec}}{E_{true}} = \frac{E_{vis}}{E_{true}} \times \frac{E_{rec}}{E_{vis}} = f_{scint}(E_{true}) \times f_{elec}(E_{vis})$$

1 Scintillator non-linearity

2 Electronics non-linearity

Scintillator Response Model

Electron response

2 parameterizations to model quenching effects and Cherenkov radiation:

1. 3-parameter purely empirical model: $$\frac{E_{\text{vis}}}{E_{\text{true}}} = \frac{1 + p_3 \cdot E_{true}}{1 + p_1 \cdot e^{-p_2 \cdot E_{\text{true}}}}$$

2. Semi-emp. model based on Birks' law: $$\frac{E_{\text{vis}}}{E_{\text{true}}} = f_{\text{q}}(E_{\text{true}}; k_B) + k_C \cdot f_c(E_{\text{true}})$$

k_B: Birks' constant
k_C: Cherenkov contribution

Gammas and positrons

- Gammas connected to electron model through MC:

$$E_{\text{vis}}^{\gamma} = \int E_{\text{vis}}^{e^-}\left(E_{\text{true}}^{e^-}\right) \cdot \frac{dN}{dE}\left(E_{\text{true}}^{e^-}\right) dE_{\text{true}}^{e^-}$$

- Positrons assumed to interact with the scintillator in same way as electrons:

$$E_{\text{vis}}^{e^+} = E_{\text{vis}}^{e^-} + 2 \cdot E_{\text{vis}}^{\gamma}(0.511\,\text{MeV})$$

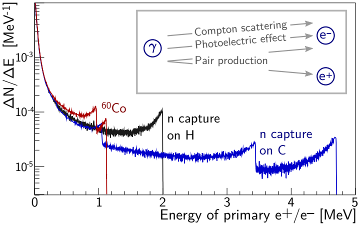

Electronics Non-Linearity Model

PMT readout electronics introduces additional biases

Electronics does not fully capture late secondary hits

⇒ Slow scintillation component missed at high energies

⇒ Charge collection efficiency decreases with visible light

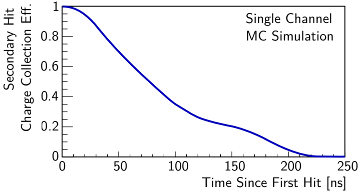

Parameterization

- Interplay of scintillation light time profile and electronics charge collection
  - ⇒ Can't be easily calibrated out on single channel level
  - ⇒ Use effective model as a function of total visible energy
- 2 empirical parameterizations: exponential and quadratic

Constraining the Non-Linearity Parameters

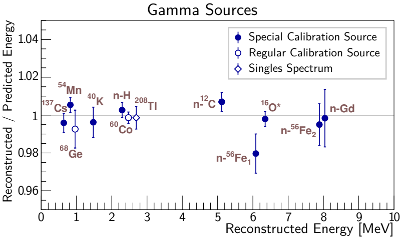

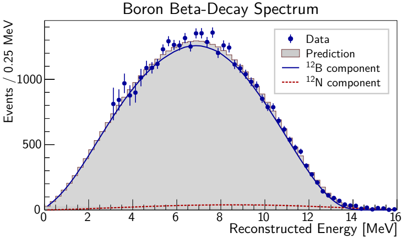

Full detector calibration data

1. Monoenergetic gamma lines from various sources
   - Radioactive calibration sources, employed regularly: ^{68}Ge, ^{60}Co, ^{241}Am^{13}C and during special calibration periods: ^{137}Cs, ^{54}Mn, ^{40}K, ^{241}Am^{9}Be, Pu^{13}C
   - Singles and correlated spectra in regular physics runs (^{40}K, ^{208}Tl, n capture on H)
2. Continuous spectrum from ^{12}B produced by muon spallation inside the scintillator

Standalone measurements

- Scintillator quenching measurements using neutron beams and Compton electrons
- Calibration of readout electronics with flash ADC

More Continuous $\beta + \gamma$ Spectra

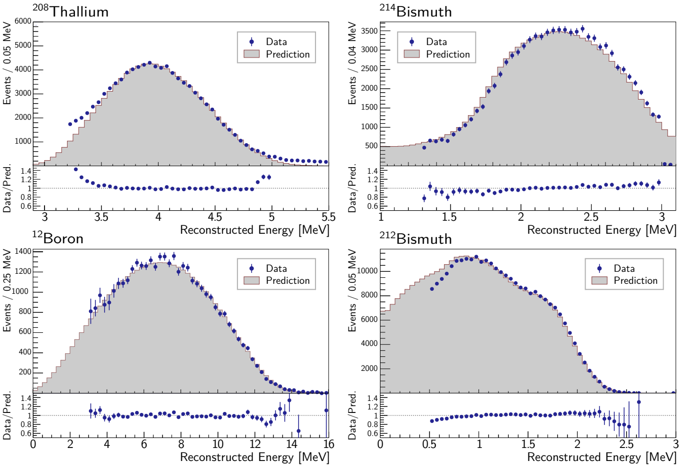

Additional spectra from ^{212}Bi, ^{214}Bi and ^{208}Tl decays

- Sizable theoretical uncertainties from 1st forbidden non-unique beta decays

  $\Rightarrow$ ^{212}Bi, ^{214}Bi and ^{208}Tl spectra only utilized to cross-check results

Final Positron Energy Non-Linearity Response

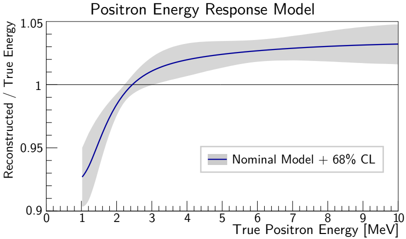

Several validated models

- Constructed based on different parameterizations/weighting of data constraints
- All models in good agreement with detector calibration data
- Resulting positron non-linearity curves consistent within $\sim 1.5\%$ uncertainty

Combination of 5 models to conservatively estimate uncertainty

- Models selected so that
  1. Correlations are minimized
  2. Remaining validated curves+uncertainties are contained in 68% C.L.
- Choice of nominal model has negligible impact on oscillation result

Energy Losses in Acrylic Vessels

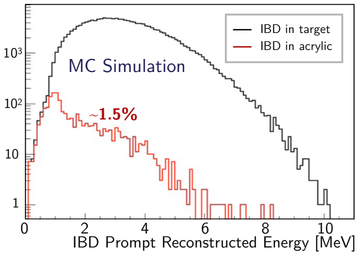

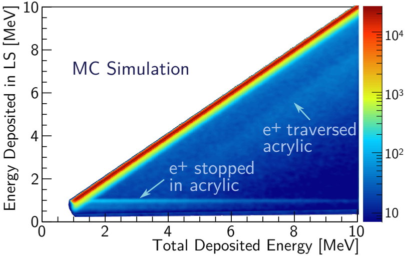

Non-scintillating inner acrylic vessels distort energy spectrum

- Kinetic energy of IBD positrons near acrylic vessels not fully detected
- Annihilation gammas with longer range can also deposit energy in vessels
- Introduces shape distortion at ~ 1 MeV
- 2D distortion matrix from MC to correct predicted positron energy spectrum

Energy Resolution Model

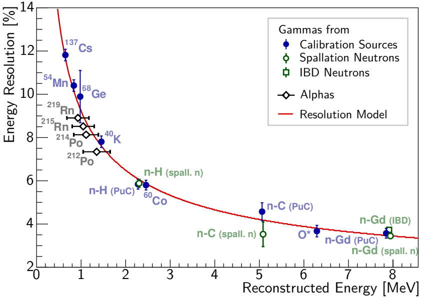

- Functional form (NIM 193, **549** (1982)):

$$\frac{\sigma_E}{E} = \sqrt{a^2 + \frac{b^2}{E} + \frac{c^2}{E^2}}$$

- Contributions from:
  1. a : Spacial/temp. resolution ($\propto E$)
  2. b : Photon statistics ($\propto \sqrt{E}$)
  3. c : Dark noise (*const.*)

Calibrated primarily using monoenergetic gamma sources

1. Radioactive calibration sources placed at the detector center
2. Additional data from IBD and spallation neutrons, uniformly distributed in LS
3. Alpha source data used to cross-check result
   $\Rightarrow$ Larger uncertainties due to different response from readout electronics

IBD Prompt Spectra

Daya Bay Near Hall

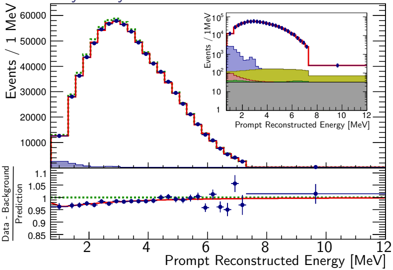

Ling Ao Near Hall

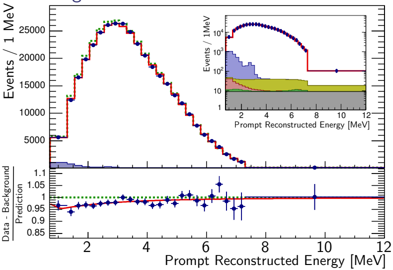

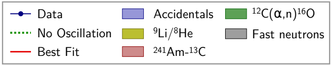

Far Hall

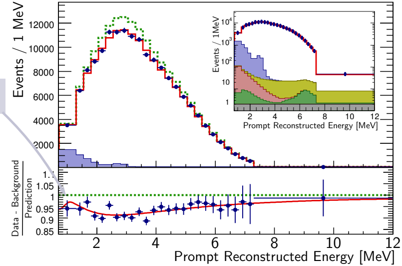

Shape distortion from energy losses in acrylic

Spectral distortion consistent with oscillation

- Both background and predicted no-oscillation spectra from best fit
- Statistical errors only

Rate+Spectra Oscillation Results

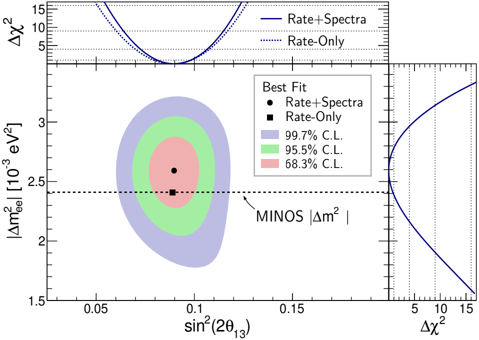

$$\sin^2 2\theta_{13} = 0.090^{+0.008}_{-0.009}$$

$$|\Delta m^2_{ee}| = 2.59^{+0.19}_{-0.20} \cdot 10^{-3}\mathrm{eV}^2$$

$$\chi^2/N_{\mathrm{DoF}} = 162.7/153$$

Strong confirmation of oscillation-interpretation of observed $\bar{\nu}_e$ deficit

	Normal MH Δm^2_{32} [10^{-3}eV^2]	Inverted MH Δm^2_{32} [10^{-3}eV^2]
From Daya Bay Δm^2_{ee}	$2.54^{+0.19}_{-0.20}$	$-2.64^{+0.19}_{-0.20}$
From MINOS $\Delta m^2_{\mu\mu}$ [João, NuFact2013]	$2.37^{+0.09}_{-0.09}$	$-2.41^{+0.12}_{-0.09}$

Pure Spectral Analysis

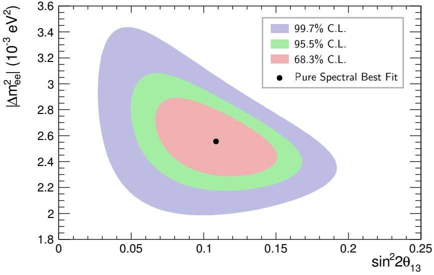

$$\sin^2 2\theta_{13} = 0.108 \pm 0.028$$

$$|\Delta m^2_{ee}| = 2.55^{+0.21}_{-0.18} \cdot 10^{-3}\mathrm{eV}^2$$

$$\chi^2/N_{\mathrm{DoF}} = 161.2/148$$

$\theta_{13} = 0$ can be excluded at $> 3\,\sigma$ from spectral information alone

- For each AD, total event prediction fixed to observed data:

  $\boxed{1}$ θ_{13} free-floating: $\chi^2/N_{\mathrm{DoF}} = 161.2/148$

  $\boxed{2}$ $\theta_{13} = 0$: $\chi^2/N_{\mathrm{DoF}} = 178.5/146$

$\Rightarrow$ $\Delta\chi^2/N_{\mathrm{DoF}} = 17.3/2$, corresponding to $p = 1.75 \cdot 10^{-4}$

Sensitivity Projection

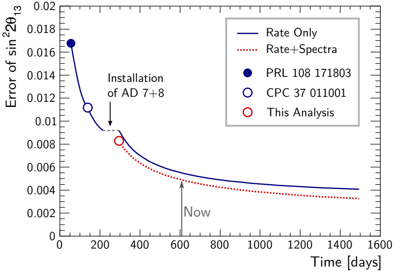

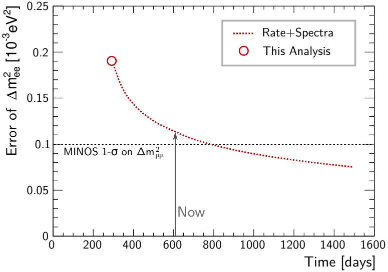

Sensitivity still dominated by statistics

- Statistics contribute $\sim 73\%$ ($\sim 65\%$) to total uncertainty in $\sin^2 2\theta_{13}$ ($|\Delta m^2_{ee}|$)
- Major systematics:

  θ_{13}: Reactor model, relative+absolute energy and relative efficiencies

  $|\Delta m^2_{ee}|$: Relative energy model, relative efficiencies and backgrounds
- Precision of mass splitting measurement closing in on results from μ flavor sector

Global Comparison of θ_{13} Measurements

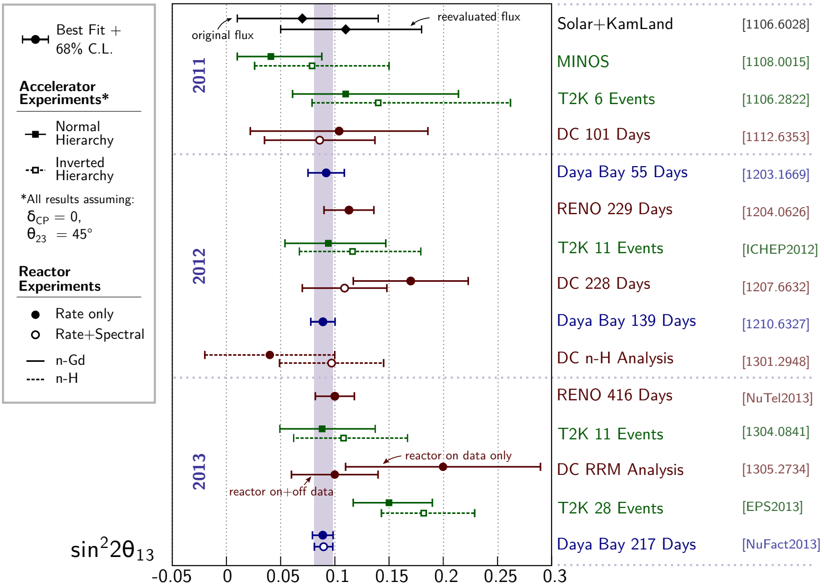

Summary

First direct measurement of the $\bar{\nu}_e$ mass-squared difference $|\Delta m^2_{ee}|$ from relative deficit and spectral distortion observed between 3 far and 3 near detectors

$$|\Delta m^2_{ee}| = (2.59\,^{+0.19}_{-0.20}) \times 10^{-3}\,\mathrm{eV}^2$$

Most precise estimate of mixing angle θ_{13} to date with 217 days of data

$$\sin^2 2\theta_{13} = 0.090\,^{+0.008}_{-0.009}$$

Expect more from Daya Bay soon:

- Measurement of the absolute reactor flux, addressing the reactor anomaly
- Constraints on non-standard neutrino models
- Significantly increased precision: 8 detectors, more than 2 years of data

Back Up

A Comment on the Mass Splitting

Short-baseline reactor experiments insensitive to mass hierarchy

- Cannot discriminate 2 frequencies contributing to oscillation: Δm^2_{31}, Δm^2_{32}
- One effective oscillation frequency Δm^2_{ee} is measured:

$$P_{\bar{\nu}_e \to \bar{\nu}_e} = 1 - \boxed{\sin^2 2\theta_{13} \sin^2\left(\Delta m^2_{ee} \frac{L}{4E}\right)} - \sin^2 2\theta_{12} \cos^4 2\theta_{13} \sin^2\left(\Delta m^2_{21} \frac{L}{4E}\right)$$

$$\sin^2(\Delta m^2_{ee} \tfrac{L}{4E}) \equiv \cos^2\theta_{12} \sin^2(\Delta m^2_{31} \tfrac{L}{4E}) + \sin^2\theta_{12} \sin^2(\Delta m^2_{32} \tfrac{L}{4E})$$

Result easily related to actual mass splitting

- Normal hierarchy $(+)$, inverted hierarchy $(-)$:

$$|\Delta m^2_{ee}| \approx |\Delta m^2_{32}| \pm 5.21 \times 10^{-3} \mathrm{eV}^2$$

- Hierarchy discrimination requires $\sim 2\%$ precision on both Δm^2_{ee} and $\Delta m^2_{\mu\mu}$

An International Effort: 230 Collaborators from 40 Institutions

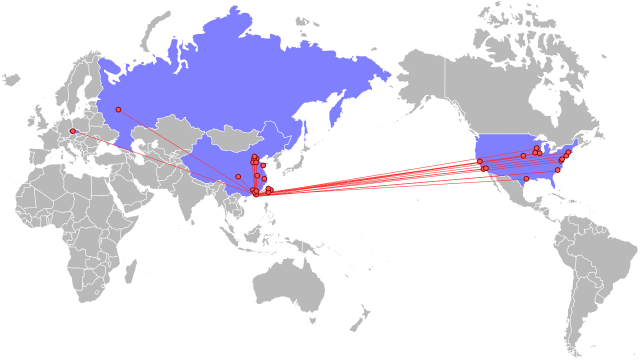

North America (17)

Brookhaven Natl Lab, CalTech, Illinois Institute of Technology, Iowa State, Lawrence Berkeley Natl Lab, Princeton, Rensselaer Polytechnic, Siena College, UC Berkeley, UCLA, Univ. of Cincinnati, Univ. of Houston, UIUC, Univ. of Wisconsin, Virginia Tech, William & Mary, Yale

Europe (2)

Charles University, JINR Dubna

Asia (21)

Beijing Normal Univ., CGNPG, CIAE, Dongguan Polytechnic, ECUST, IHEP, Nanjing Univ., Nankai Univ., NCEPU, Shandong Univ., Shanghai Jiao Tong Univ., Shenzhen Univ., Tsinghua Univ., USTC, Xian Jiaotong Univ., Zhongshan Univ., Chinese Univ. of Hong Kong, Univ. of Hong Kong, Na2onal Chiao Tung Univ., Na2onal Taiwan Univ., Na2onal United Univ.

Antineutrino Detection via Inverse Beta Decay

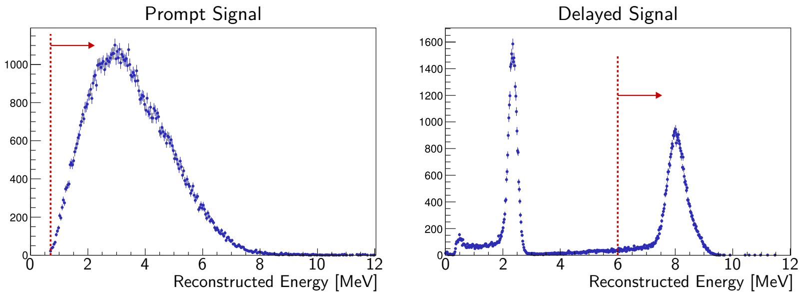

Prompt+delayed coincidence provides distinctive signature

$$\bar{\nu}_e + p \rightarrow e^+ + n \qquad \textit{prompt}$$

$$\hookrightarrow + p \xrightarrow{\tau \approx 200\ \mu s} D + \gamma \qquad (2.2\,\text{MeV})$$

$$\hookrightarrow + Gd \xrightarrow{\tau \approx 28\ \mu s} Gd^* \rightarrow Gd + n\gamma \qquad (8\,\text{MeV}) \qquad \textit{delayed}$$

- Neutrino energy: $E_{\bar{\nu}_e} \approx T_{e^+} + T_n + (m_n - m_p) + m_{e^+} \approx T_{e^+} + 1.8\,\text{MeV}$
- Higher energy and shorter capture time on Gd improve background rejection

Antineutrino Detector (AD) Design

8 functionally identical detectors
reduce systematic uncertainties

3 zone cylindrical vessels

	Liquid	Mass	Function
Inner acrylic	Gd-doped liquid scint.	20 t	Antineutrino target
Outer acrylic	Liquid scintillator	20 t	Gamma catcher
Stainless steel	Mineral oil	40 t	Radiation shielding

192 8 inch PMTs in each detector

Top and bottom reflectors increase light yield
and flatten detector response

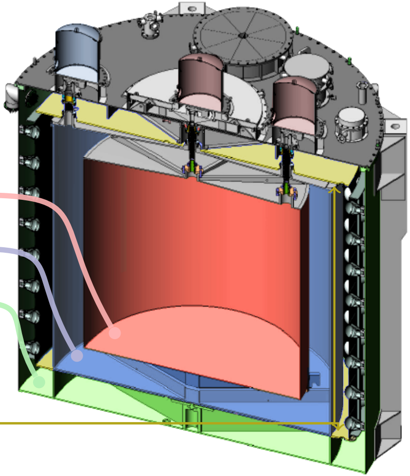

Antineutrino (IBD) Selection

Use IBD prompt+delayed coincidence signal

1. Reject spontaneous PMT light emission ("flashers")
2. Prompt positron:
   $0.7\,\text{MeV} < E_p < 12\,\text{MeV}$
3. Delayed neutron:
   $6.0\,\text{MeV} < E_d < 12\,\text{MeV}$
4. Neutron capture time:
   $1\,\mu\text{s} < \Delta t < 200\,\mu\text{s}$
5. Muon veto:
   - Water pool muon (>12 hit PMTs):
     Reject $[-2\mu\text{s}, 600\mu\text{s}]$
   - AD muon (>20 MeV):
     Reject $[-2\mu\text{s}, 1400\mu\text{s}]$
   - AD shower muon (>2.5 GeV):
     Reject $[-2\mu\text{s}, 0.4\text{s}]$
6. Multiplicity:
   - No additional prompt-like signal
     $400\mu\text{s}$ before delayed neutron
   - No delayed-like signal
     $200\mu\text{s}$ after delayed neutron

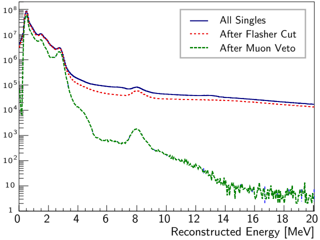

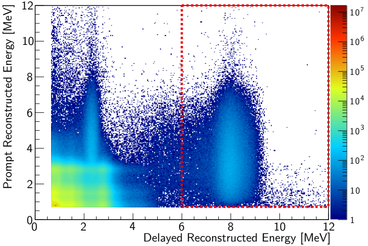

Summary of Uncertainties

	Detector		
	Efficiency	Correlated	Uncorrelated
Target Protons		0.47%	0.03%
Flasher cut	99.98%	0.01%	0.01%
Delayed energy cut	90.9%	0.6%	0.12%
Prompt energy cut	99.88%	0.10%	0.01%
Multiplicity cut		0.02%	<0.01%
Capture time cut	98.6%	0.12%	0.01%
Gd capture ratio	83.8%	0.8%	<0.1%
Spill-in	105.0%	1.5%	0.02%
Livetime	100.0%	0.002%	<0.01%
Combined	**78.8%**	**1.9%**	**0.2%**

Reactor			
Correlated		Uncorrelated	
Energy/fission	0.2%	Power	0.5%
IBD/fission	3%	Fission fraction	0.6%
		Spent fuel	0.3%
Combined	3%	**Combined**	**0.8%**

Summary of Uncertainties

	Detector		
	Efficiency	Correlated	Uncorrelated
Target Protons		0.47%	0.03%
Flasher cut	99.98%	0.01%	0.01%
Delayed energy cut	90.9%	0.6%	0.12%
Prompt energy cut	99.88%	0.10%	0.01%
Multiplicity cut		0.02%	<0.01%
Capture time cut	98.6%	0.12%	0.01%
Gd capture ratio	83.8%	0.8%	<0.1%
Spill-in	105.0%	1.5%	0.02%
Livetime	100.0%	0.002%	<0.01%
Combined	**78.8%**	**1.9%**	**0.2%**

- Only uncorrelated uncertainties relevant to near/far oscillation analysis

Reactor			
Correlated		Uncorrelated	
Energy/fission	0.2%	Power	0.5%
IBD/fission	3%	Fission fraction	0.6%
		Spent fuel	0.3%
Combined	3%	**Combined**	**0.8%**

Summary of Uncertainties

	Detector		
	Efficiency	Correlated	Uncorrelated
Target Protons		0.47%	0.03%
Flasher cut	99.98%	0.01%	0.01%
Delayed energy cut	90.9%	0.6%	0.12%
Prompt energy cut	99.88%	0.10%	0.01%
Multiplicity cut		0.02%	$<$0.01%
Capture time cut	98.6%	0.12%	0.01%
Gd capture ratio	83.8%	0.8%	$<$0.1%
Spill-in	105.0%	1.5%	0.02%
Livetime	100.0%	0.002%	$<$0.01%
Combined	**78.8%**	**1.9%**	**0.2%**

- Only uncorrelated uncertainties relevant to near/far oscillation analysis
- Largest systematics smaller than far site statistics ($\sim$ 1%)

Reactor			
Correlated		Uncorrelated	
Energy/fission	0.2%	Power	0.5%
IBD/fission	3%	Fission fraction	0.6%
		Spent fuel	0.3%
Combined	3%	**Combined**	**0.8%**

Summary of Uncertainties

	Detector		
	Efficiency	Correlated	Uncorrelated
Target Protons		0.47%	0.03%
Flasher cut	99.98%	0.01%	0.01%
Delayed energy cut	90.9%	0.6%	0.12%
Prompt energy cut	99.88%	0.10%	0.01%
Multiplicity cut		0.02%	<0.01%
Capture time cut	98.6%	0.12%	0.01%
Gd capture ratio	83.8%	0.8%	<0.1%
Spill-in	105.0%	1.5%	0.02%
Livetime	100.0%	0.002%	<0.01%
Combined	**78.8%**	**1.9%**	**0.2%**

- Only uncorrelated uncertainties relevant to near/far oscillation analysis
- Largest systematics smaller than far site statistics ($\sim$ 1%)

Reactor			
Correlated		Uncorrelated	
Energy/fission	0.2%	Power	0.5%
IBD/fission	3%	Fission fraction	0.6%
		Spent fuel	0.3%
Combined	3%	**Combined**	**0.8%**

- Impact of uncorrelated reactor systematics reduced by relative measurement

Reactor Flux Models

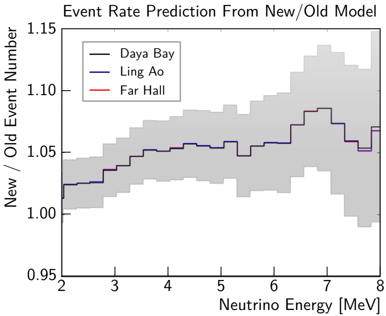

	Ratio of $\bar{\nu}_e$ from isotope [%]			
	^{235}U	^{238}U	^{239}Pu	^{241}Pu
AD 1	63.3	12.2	19.5	4.8
AD 2	63.3	12.2	19.5	4.8
AD 3	61.0	12.5	21.5	4.9
AD 4	61.5	12.4	21.5	4.9
AD 5	61.5	12.4	21.5	4.9
AD 6	61.5	12.4	21.5	4.9

Flux model has negligible impact on oscillation measurement

- Flux from each reactor used to predict IBDs at each detector

  1. New model:
     - P. Huber, Phys. Rev. C84, 024617 (2011),
     - T. Mueller et al., Phys. Rev. C83, 054615 (2011)
  2. Old model:
     - A. A. Hahn et al., Phys Rev Lett. B218, 365 (1989)
     - P. Vogel et al. Phys. Rev. C24, 1543 (1981)
     - K. Schreckenbach et al., Phys. Lett. B160, 325 (1985)

Construct Energy Response Model from Calibration Data

3 Basic Approaches

1. Method 1
   - No constraints on scintillation model from bench data
   - Any combination of parameterizations for scintillator and electronics
   - All parameters determined by simultaneous fit to ^{12}B and gamma data
   - Cross-check with remaining 3 continuous $\beta + \gamma$ spectra
2. Method 2
   - Semi-empirical model based on Birks' law quenching for scintillation response
   - Birks constant and Cherenkov contribution constrained by bench measurements
   - Electronics response from quadratic fit to gamma data
   - Cross-check with all 4 continuous $\beta + \gamma$ spectra
3. Method 3
   - Semi-empirical model for scintillation response
   - Birks constant constrained by bench measurements
   - Cherenkov contribution and electronics from exponential fit to all 4 $\beta + \gamma$ spectra
   - Cross-check with gamma data

Comparison of best fit models

- 12 models based on 3 basic methods with different weighting of input data
- All models in good agreement with AD calibration data
- Resulting positron non-linearity curves consistent within $\sim 1.5\%$ uncertainty

Three Neutrino Oscillation: PMNS Matrix

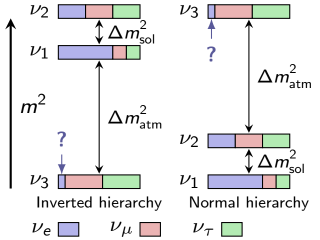

Weak and mass eigenstates need not correspond:

1. How they interact
2. How they propagate

$\alpha = e, \mu, \tau$

$$|\nu_\alpha\rangle = \sum_{i=1}^{3} U_{\alpha,i} \, |\nu_i\rangle$$

θ_{13} only recently well established by Daya Bay

$$U = \begin{pmatrix} 1 & 0 & 0 \\ 0 & \cos\theta_{23} & \sin\theta_{23} \\ 0 & -\sin\theta_{23} & \cos\theta_{23} \end{pmatrix} \begin{pmatrix} \cos\theta_{13} & 0 & \sin\theta_{13} e^{-i\delta} \\ 0 & 1 & 0 \\ -\sin\theta_{13} e^{i\delta} & 0 & \cos\theta_{13} \end{pmatrix} \begin{pmatrix} \cos\theta_{12} & \sin\theta_{12} & 0 \\ -\sin\theta_{12} & \cos\theta_{12} & 0 \\ 0 & 0 & 1 \end{pmatrix}$$

- $\theta_{23} \sim 45^\circ$ established through atmosperic+accelerator experiments: possibly maximal
- $\theta_{12} \sim 34^\circ$ established through solar experiments and KamLAND: large but not maximal

The Daya Bay Strategy

Relative measurement with 8 functionally identical detectors

- Absolute reactor flux single largest uncertainty in previous measurements

$\Longrightarrow$ Cancels in near/far ratio: $\frac{N_\mathrm{f}}{N_\mathrm{n}} = \left(\frac{N_{p,\mathrm{f}}}{N_{p,\mathrm{n}}}\right)\left(\frac{L_\mathrm{n}}{L_\mathrm{f}}\right)^2\left(\frac{\epsilon_\mathrm{f}}{\epsilon_\mathrm{n}}\right)\left(\frac{P_\mathrm{sur}(E,L_\mathrm{f})}{P_\mathrm{sur}(E,L_\mathrm{n})}\right)$

Baseline optimization

- Detector locations optimized to known parameter space of $|\Delta m^2_{ee}|$
- Far site maximizes term dependent on $\sin^2 2\theta_{13}$

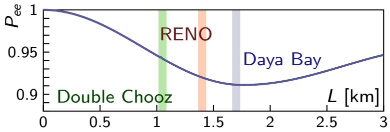

Go strong, big and deep!

	Reactor [GWth]	Target [t]	Depth [m.w.e]
Double Chooz	8.6	16 (2×8)	300, 120 (far, near)
RENO	16.5	32 (2×16)	450, 120
Daya Bay	17.4	160 (8×20)	860, 250
	Lots of signal		Little background

Daya Bay: A Powerful Neutrino Source at an Ideal Location

Among the top 5 most powerful reactor complexes in the world, 6 cores produce 17.4 GW$_{th}$ power, 35×10^{20} neutrinos per second